View metadata, citation and similar papers at core.ac.uk

brought to you by CORE

provided by Loughborough University Institutional Repository

This item was submitted to Loughborough's Institutional Repository (https://dspace.lboro.ac.uk/) by the author and is made available under the following Creative Commons Licence conditions.

creative commons

COMMONS DEED

Attribution-NonCommercial-NoDerivs 2.5

You are free:

- to copy, distribute, display, and perform the work

Under the following conditions:

Attribution. You must attribute the work in the manner specified by the author or licensor.

Noncommercial. You may not use this work for commercial purposes.

No Derivative Works. You may not alter, transform, or build upon this work.

- For any reuse or distribution, you must make clear to others the license terms of this work.
- Any of these conditions can be waived if you get permission from the copyright holder.

Your fair use and other rights are in no way affected by the above.

This is a human-readable summary of the Legal Code (the full license).

Disclaimer

For the full text of this licence, please go to:
http://creativecommons.org/licenses/by-nc-nd/2.5/

Stirred cell membrane emulsification for multiple emulsions containing unrefined pumpkin seed oil with uniform droplet size

Marijana M. Dragosavac[a], Richard G. Holdich[a,b], Goran T. Vladisavljević[a,c] and Milan N. Sovilj[d]

[a]Chemical Engineering Department, Loughborough University, Loughborough, Leicestershire LE11 3TU, UK

[b]Micropore Technologies Ltd., The Innovation Centre, Epinal Way, Loughborough, Leicestershire LE11 3EH, UK

[c]Vinča Institute of Nuclear Sciences, PO Box 522, RS-11001 Belgrade, Serbia

[d]Faculty of Technology, Department of Chemical Engineering, University of Novi Sad, Bul. Cara Lazara 1, RS-21000 Novi Sad, Serbia

Abstract

Stirred cell membrane emulsification, using flat metal discs with pore sizes between 15 and 40 μm, were used to create double emulsions of water-in-oil-in-water droplets. The oil phase was a lipid, most often unrefined pumpkin seed oil, with a few comparative tests using sunflower oil. The drops contained an internal water phase of 30% by volume and oil fluxes of up to 3200 L m^{-2} h^{-1} were used. The drops were stabilized using 2% Tween 20 (polyoxyethylene sorbitan monolaurate), or 2% Pluronic F-68 (polyoxyethylene-polyoxypropylen copolymer) as the outer aqueous surfactant solution. Median drop sizes were in the range between 100 and 430 μm, depending on the process conditions: mainly shear at the membrane surface and dispersed phase injection rate. In most cases the drops were very uniform, with span

(i.e. 90% drop size minus 10% drop size divided by median size) values of around 0.5. This data is similar to what was obtained previously for simple O/W emulsions of the same materials. Hence, the internal water phase, and internal surfactant, 5% PGPR (polyglycerol polyricinoleate), did not adversely influence the emulsification process. A marker material, copper sulfate, was added to the internal water phase and the release of copper was monitored with respect to time. For both lipid systems, at the larger droplet size, there was a significant period of no copper release, followed by almost linear release with time. This initial period was absent when the drop size was close to 100 μm. The initial entrapment efficiency of the copper, in all experiments, was higher than 94%.

Keywords: Membrane emulsification; stirred cell; pumpkin seed oil; multiple emulsions; encapsulation efficiency.

1. Introduction

Multiple emulsions [1] have attracted significant interest in the past several decades. They have potential applications in the pharmaceutical industry, such as carriers of active pharmaceutical ingredients, e.g. in drug delivery systems [2]; cosmetics, e.g. deposition of water soluble benefit agents onto skin [3]; and the food industry, e.g. encapsulation of flavours [4, 5], production of food with lower fat content [6] and protection of sensitive and active food components from a local harsh environment [7]. Multiple emulsions are very suitable for encapsulation of hydrophilic bioactive components, such as: vitamin B [8], immunoglobulin [9], insulin [10] and amino acids [8, 11], and they are also useful for preparation of delivery systems that contains

lipophilic encapsulants, such as flavour [12] and both lipophilic and hydrophilic bioactive components in the same system [8].

Multiple emulsions are complex systems where both water-in-oil (W/O) and oil-in-water (O/W) emulsion types exist simultaneously [13]. Water-in-oil-in-water (W/O/W) emulsions contain small primary water droplets within larger oil droplets while the oil droplets are dispersed within the secondary continuous water phase. In the second step of the emulsification process, when the W/O/W droplets are produced, carefully controlled shear needs to be applied as there is a requirement not to rupture the primary emulsion [14], which would lead to a lowering of the encapsulation efficiency. Also, many ingredients suitable for multiple emulsions are temperature and shear sensitive, and application of high shear would lead to deterioration in their properties [15]. Membrane emulsification (ME) can be used to prepare emulsions, with low mechanical stress [16] or even without any shear [17], at a low energy input compared with conventional emulsification methods and with better control of droplet size [18]. Crossflow ME, where dispersed phase is pressed through the microporous membrane while continuous phase flows along the membrane surface, is not convenient for production of larger droplets, typically over 15 μm, due to the need to recycle the dispersion over the membrane surface leading to damage to the previously formed drops within the pump and fittings of the system [19]. Larger diameter drops are appropriate for controlled release applications, or encapsulations, in food supplements and for crop nutrients and are often a precursor to the formation of a complex coacervate encapsulated particle.

Unrefined pumpkin seed oil is particularly rich in omega-3 fatty acids [20] and tocopherol [21] and should be emulsified under low shear conditions to avoid heating and lipid oxidation. Pumpkin seed oil has a rich flavour which is easily lost if heated, therefore, membrane emulsification seems to be a very convenient technique for production of emulsions of unrefined pumpkin seed oil of high biological value and desired organoleptic properties.

Other related methods of producing W/O/W emulsions include microfabricated channel arrays [22-24], T-junction [25] and flow focusing channels [26]. These techniques can provide exceptionally uniform droplets and high encapsulation efficiency, but in all cases they have very low productivity (1 to 10 mL per hour at pore sizes equivalent to the work reported here) restricting their use to laboratory investigation of formulation conditions. They do not provide a readily scalable technique for commercial production. A previous study using stirred cell emulsification of single emulsions of unrefined pumpkin seed oil, and refined sunflower oil, using the Micropore Technologies Dispersion Cell [27] demonstrated the feasibility of the technique. Scaling from the stirred cell approach to an oscillating membrane system was also demonstrated [28], whereby it would be possible to provide greater membrane area for commercial applications.

The aim of this work was to investigate the influence of the internal phase content, shear at the membrane, membrane pore size, and flux through the membrane on the production of multiple emulsions using a metal disc membrane in the Dispersion Cell. The encapsulation efficiency of a marker (copper salt) was also investigated. To predict the droplet size a model introduced in previous work for simple emulsions

[27] was used. The droplet diameter x is calculated from a force balance of the capillary force (function of interfacial tension and pore size) and the drag force (function of a shear stress and the droplet size) acting on a strongly deformed droplet at a single membrane pore:

$$x = \frac{\sqrt{18\tau_{av}{}^2 r_p^2 + 2\sqrt{81\tau_{av}{}^4 r_p^4 + 4r_p^2 \tau_{av}{}^2 \gamma^2}}}{3\tau_{av}} \quad (1)$$

where r_p is the pore radius, τ_{av} is the average shear stress, γ is the interfacial tension and x is the formed droplet diameter. The average shear over the whole membrane area is given by:

$$\tau_{av} = \frac{\int_0^{r_{trans}} 0.825\mu\omega r \frac{1}{\delta}(2\pi r)dr + \int_{r_{trans}}^{D_m/2} 0.825\mu\omega r_{trans}\left(\frac{r_{trans}}{r}\right)^{0.6} \frac{1}{\delta}(2\pi r)dr}{\pi D_m^2 / 4} \quad (2)$$

where D_{m} is the effective diameter of the membrane, i.e. the diameter exposed to the continuous phase, r_{trans} is transitional radius (where the shear stress reaches the maximal value) [27], r is distance from the membrane centre, ρ is the continuous phase density, ω is the angular velocity, μ is the continuous phase coefficient of dynamic viscosity and δ is boundary layer thickness $\delta = \sqrt{\mu/\omega\rho}$.

For the purposes of modelling the release of an encapsulated species a diffusion based model was assumed:

$$\frac{\partial q}{\partial t} = \frac{1}{r_x^2}\frac{\partial}{\partial r_x}\left(D_{eff} \cdot r_x^2 \frac{\partial q}{\partial r_x}\right) \quad (3)$$

where q is the concentration of the encapsulated species expressed as grams of species encapsulated divided by grams of total particle, t is time, r_x is the radial position within the particle (or W/O/W composite drop) and D_{eff} is the 'effective' diffusion

coefficient for the transferring species within the drop. At the start of the release period, the concentration of the encapsulated species in the surrounding water phase is zero and it is assumed to remain negligible; providing one boundary condition for the solution of equation (3) together with a differential lower boundary where:

$$\frac{\partial q}{\partial r}_{|r=0} = 0$$

which is a statement that the concentration of the transferring species is symmetrical within the drop/particle, in spherical polar coordinates, around the origin of the drop. Equation (3) can be solved numerically for the concentration of the encapsulated species with both radial position and time using these boundary conditions and an initial condition based on a knowledge of the total mass of encapsulated species within the drop, which is assumed to be uniformly distributed at the start of the release process. A material balance can be used to calculate the mass of encapsulated species leaving the drop/particle and, therefore, the resulting concentration of the species within the exterior water phase, which may then be used to predict the variation of encapsulation efficiency with time (i.e. the release profile).

2. Experimental

2.1. Materials

The oil phase (O) in $W_1/O/W_2$ emulsions was 5 wt.% PGPR (polyglycerol polyricinoleate from Stepan Limited, UK) dissolved in unrefined pumpkin seed oil (density of 913 kg m^{-3} at 298 K kindly donated by GEA Tovarna Olja, Slovenia) or refined sunflower oil (food grade from a local supermarket). The inner aqueous phase (W_1) was pure (demineralised) water. Where appropriate, the inner water phase contained 2000 ppm $CuSO_4$ (copper sulphate, Fisher Scientific, UK) to investigate encapsulation efficiency. The outer aqueous phase (W_2) for stabilising the W_1/O

emulsion contained 2 wt.% Tween® 20 (polyoxyethylene sorbitan monolaurate from Fluka, UK). The formulation of the product emulsions and the range of particle sizes obtained are listed in Table 1. The density of oil and continuous phase was measured using an Anton Paar digital density meter (model DMA 46, Graz, Austria). The oil viscosity was measured using HAAKE RheoStress® model RS600 rheometer with sensor C60/1° Ti and a gap of 51 μm (Thermo Electron, Karlsruhe, Germany). The continuous phase viscosities were measured with a Cannon-Ubbelohde model 9721-K50 viscometer (CANNON® Instrument Company, USA). The equilibrium interfacial tensions at the oil/water interface were measured by the Du Nouy ring method using a White Electric Instrument tensiometer (model DB2KS). The physical properties of the surfactant solutions and the equilibrium interfacial tensions for the two different oils used are listed in Table 2.

2.2. Membranes and membrane module

The emulsions were obtained using a Dispersion Cell with a flat disc membrane under the paddle blade stirrer, as shown in Fig. 1. Both Dispersion Cell and membranes were supplied by Micropore Technologies Ltd. (Loughborough, UK). The agitator was driven by a 24 V DC motor and power supply (INSTEK Model PR 3060) and paddle rotation speed in the range from 3.8 to 25 Hz (230 to 1500 rpm) was controlled by the applied voltage. The membranes used were nickel membranes containing uniform cylindrical pores with a diameter of 10, 20, 30 or 40 μm and a pore spacing of 200 μm. The porosity of the membranes [37] was 0.2, 0.9, 2 and 3.6%, respectively. A perfectly ordered hexagonal array of pores with a pore at the centre of each hexagonal cell can be seen on the micrograph in Fig. 1.

2.3. Experimental procedure

$W_1/O/W_2$ emulsions were prepared by a two-step emulsification procedure. The W_1/O emulsion was prepared by means of a homogeniser (Ultra Turrax®, model T25, IKA Works, USA) at 24,000 rpm for 5 min which ensured that the mean droplet size of inner oil droplets was about 0.5 μm [29]. The W_1/O emulsion was injected through the membrane (pre-soaked in a proprietary wetting agent for at least 30 min to increase the hydrophilicity of the surface) using a peristaltic pump (Watson-Marlow-Bredel Pump 101U/R, Cornwall, UK) at the constant flow rate of 0.5–50 mL min^{-1}, corresponding to the dispersed phase fluxes of 30–3200 L m^{-2} h^{-1}. Rotation speed of the stirrer placed on top of the membrane ranged from 230 to 1330 rpm (equal to shear stresses between 1 to 18 Pa [27]). The initial volume of surfactant solution in the cell was 125 cm^3 and the experiments were run until the dispersed phase concentration reached 5 vol.%. Once the desired amount of oil had passed through the membrane, both the pump and the agitator were switched off and the droplets were collected and analyzed. The membrane was cleaned with 8 M NaOH in an ultrasonic bath for 5 min followed by treatment in 10 vol.% HCl solution for 5 min. To evaluate the drop-size distribution and droplet diameter, a laser diffraction particle size analyzer (Malvern Mastersizer, Model S) was used. For each emulsion, three separate samples and measurements were performed and the mean average of these is reported. The particle size was expressed as the volume median diameter $d(v,0.5)$, which is the diameter corresponding to 50 vol.% on the cumulative distribution curve. The relative span of a drop size distribution was used to express the degree of drop size uniformity: span=$[d(v,0.9)-d(v,0.1)]/d(v,0.5)$. Photomicrographs of the prepared emulsions were also taken, to confirm the droplet size reported by Malvern

Mastersizer S. The photomicrographs of membrane surface and emulsions were taken using a Leitz Ergolux optical microscope.

2.4. Measurement of encapsulation efficiency of the marker substance

For measuring the encapsulation efficiency of the internal water phase (W_1) $CuSO_4.6H_2O$ (Sigma-Aldrich Company Ltd., UK) was dissolved giving a Cu concentration of 2000 ppm. The encapsulation efficiency was determined by separating the W_1/O drops from the outer water phase using disposable Vivaspin centrifugal ultrafilters (Sartorius AG, Goettingen, Germany). These ultrafilters are equipped with polyethersulfone (PES) membranes with a mean pore size of 0.2 μm and effective area of 2.5 cm^2. Ultrafiltration was carried out at 1300 rpm for 40 min using a Heraeus Labofuge 400R centrifuge (Thermo Scientific, Germany). Cu concentration in the filtrate was then measured using an Atomic Absorbance Spectrophotometer (AAS) (Spectra AA-200 Varian, UK).

The encapsulation efficiency (Y) was expressed as the fraction of copper that remained encapsulated within the water droplets after multiple emulsion production [38]:

$$Y = \frac{M_i - M_e}{M_i} \tag{4}$$

where M_i is the mass of copper initially present in the internal water droplets in the W/O emulsion and M_e is the mass of copper present in the external water phase in the W/O/W emulsion after homogenization.

The encapsulation efficiency is calculated by assuming that the amount of copper released from the inner water droplets is proportional to the amount of water released

and that the copper is released due to expulsion of the internal water droplets during formation of the W/O/W emulsion, or with time during release profile studies. The mass of copper initially present in the internal water droplets in the W/O emulsion is then given by

$$M_i = C_i V_i = C_i \times \phi_{WO} \times \phi_{WOW} \times V_{WOW} \quad (5)$$

The mass of copper present in the external water phase in the W/O/W emulsion after emulsification is then given by [30]

$$M_e = C_e\left[V_e + (1-Y)\times V_i\right] = C_e \times V_e\left[(1-\phi_{WOW}) + (1-Y)\times \phi_{WO} \times \phi_{WOW}\right] \quad (6)$$

Here, C_i is the copper concentration in the internal aqueous phase of the W/O emulsion and C_e is the copper concentration measured in the external aqueous phase of the $W_1/O/W_2$ emulsion after emulsification. V_i, V_e, and V_{WOW} are the volume of the internal water phase used to prepare the W_1/O emulsion, the volume of the external water phase used to prepare the $W_1/O/W_2$ emulsion, and the volume of the overall emulsion, respectively. In addition, ϕ_{WO} is the volume fraction of water droplets in the W_1/O emulsion, whereas ϕ_{WOW} is the volume fraction of W/O droplets in the W/O/W emulsion. Substitution of Eqs. 5 and 6 into Eq. 4 gives [30]

$$Y = 1 - \frac{C_e}{C_i - C_e}\left(\frac{1-\phi_{WOW}}{\phi_{WOW} \times \phi_{WO}}\right) \quad (7)$$

In this study, the encapsulation efficiency is expressed as a percentage. For the particular system used in this study, C_i = 0.2% w/v, ϕ_{WO} = 0.3, and ϕ_{WOW} = 0.05. Hence, the encapsulation efficiency is given by the following approximate expression: % $Y = 100 \times (1 - 316.67C_e / [1 - 5C_e])$, when C_i and C_e are expressed in % w/v.

3. Results and discussion

Fig. 2 shows the effect of dispersed phase flux on the droplet size for four different rotational speeds using the 20 μm membrane with 200 μm pore spacing, and single set of data using the 40 μm membrane at the same pore spacing, with increasing transmembrane flux up to 3200 L m^{-2} h^{-1}. Droplets produced at high rotation speed (high shear stress) had smaller drop diameter than the ones produced at low rotation speed (low shear stress) which is in agreement with the literature [18, 27-29]. As can be seen from Fig. 2 in the case when rotation speed was 230 rpm droplets greater than 300 μm were formed, which is considerably larger than the spacing between the pores. Therefore, the drops on the membrane surface would need to deform before detachment, and it may be that not all pores of a membrane are active [31], providing more space for droplets to grow on the membrane. Fig. 2 shows that uniform droplets with span values less than 0.5 were obtained for almost all fluxes except the extreme cases of very low, and very high, rotation speed and high transmembrane flux, where some drop beak-up after formation is likely. In this work a maximum transmembrane flux of 3200 L m^{-2} h^{-1} was achieved, and the lowest span was 0.46 when the stirrer had a rotation speed of 960 rpm. When a 40 μm membrane was used, under identical shear conditions, droplets were ~1.3 times bigger than those produced using 20 μm membrane. The data illustrates that large W/O/W droplets are achievable, even at high dispersed phase injection rates, with span values that are similar to the simple emulsion (O/W) values of 0.46. Also included on this figure is the predicted drop size using the model, equation (1), which is marked at the point where the transmembrane flux is equal to zero: as the model does not account for flux rate. Clearly, increasing flux increases produced drop size. Further discussion of the model is provided later when considering shear stress.

Unrefined pumpkin seed oil is rich in many compounds that can be adsorbed on the membrane surface, such as free fatty acids, minerals, phospholipids, chlorophyll, and aromatic components. The adsorption of these components as well as molecules of PGPR on the membrane surface may lead to membrane wetting by the oil phase. Such interactions could cause alteration of the membrane surface from hydrophilic to hydrophobic [32]. Therefore, Tween 20 and Pluronic F68 were used as water soluble surfactants, as they are both nonionic surfactants with no affinity to adsorb to the membrane surface. In order to determine the effect of internal water phase and effect of PGPR molecules on the membrane surface and the droplet size four different tests were performed using a membrane with 15 μm pores and 200 μm pore spacing, and the results are presented in the Fig. 3. After each experiment the membrane was ultrasonically treated for 5 min in NaOH, then dried, followed by ultrasonication for 5 min in 10% HCl and dried again. After washing in the base and acid the membrane was left in the wetting agent for 1h. In all experiments 2% Pluronic F68 was used as the continuous phase.

In the first experiment pure pumpkin seed oil was used as the dispersed phase. The experiment was repeated three times and the average value for *d(v,0.5)* is presented the error bars indicating the highest and the lowest values obtained. *d(v,0.1)* and *d(v,0.9)* are presented for information in Fig. 3. The average droplet size produced using the fresh membrane was 124 μm and the reproducibility of the experiment was good (see Fig. 3). The image shown above the first set of histogram bars shows the almost transparent droplets of pure pumpkin seed oil injected into the continuous phase. In the second experiment 5% of PGPR was dissolved in the oil phase, but no internal water phase was present. Again experiments were repeated three times and

the average value is presented for *d(v,0.5)*, the error bars indicate the highest and the lowest values obtained. The average droplet size when the PGPR was dissolved in oil was 126 μm, an insignificant difference to when no PGPR was used. From the image provided above the set of histograms above item 2, it is notable that the presence of PGPR made the drops slightly darker, but still translucent. The third experiment, reported in Fig 3, involved the use of an inner water phase stabilised by PGPR. Again three experiments were conducted and the average value for *d(v,0.5)* is reported and error bars present the highest and the lowest values obtained. The image of the drops now shows complete light obscuration, as would be expected due to complete light scattering within the drop. This contrasts significantly with the previous images of drops containing just PGPR stabiliser and pumpkin seed oil, and just the pumpkin seed oil. From Fig. 3, for the W/O/W emulsion, it can be seen that the median droplet size increases by approximately 20 μm. Such increase may be due to wetting of the membrane and the final test was performed to see if this is irreversible. In the final experiment the pure pumpkin seed oil was used again as dispersed phase. As it can be seen from Fig. 3 the droplet size was no different from the first experiment showing that the cleaning of the membrane was efficient.

Another factor that may influence the drop size being formed during membrane emulsification is the viscosity of the dispersed phase, which is likely to be greater for the W/O_p dispersion, as well as the ability of the surfactant to stabilise the emerging oil drop. All the interfacial tensions reported in Table 2 are equilibrium values, and it is possible that a dynamic interfacial tension may be more relevant, if the rate of diffusion of the stabilising molecules to the emerging drop is low. An analysis of the droplet formation time was performed for a flux rate of 2000 l m^{-2} h^{-1} using a 20 μm

pore size membrane. The drop formation time varied from 0.3 to 0.5 seconds depending on whether 10 to 18% of the available pores were generating drops. Following the analysis of van der Graaf et al [33], these times correspond to a region where the rate of increase in interfacial area will be low, but there may still be a slight increase in interfacial tension over the equilibrium value and, therefore, increased drop size. The effective diffusion coefficient of Pluronic F68 is reported as 1.9×10^{-11} m^2 s^{-1} [34] while for Tween 20 Luschtinetz and Dosche reported a value of 7.7×10^{-11} m^2 s^{-1} [35]. Since the loading of the interface with surfactant is directly proportional to the effective diffusion coefficient [33], it will take longer for Pluronic F68 molecules to stabilise the forming oil droplet which may also explain the larger diameters presented in Fig. 4 and the slightly poorer span values. With increase of transmembrane flux from 2550 L m^{-2} h^{-1} to 3200 L m^{-2} h^{-1}, when the continuous phase included 2% Pluronic F68, droplet size increased from 279 to 303 μm but the span reduced from 0.76 to 0.54.

Fig. 5 demonstrates the influence of the rotation speed on the droplet size for multiple emulsions of pumpkin seed oil at various flux rates. As found earlier for single emulsions [27], mean droplet size decreases with increasing shear stress. The shear stress on the membrane surface does depend on the distance from the axis of rotation and reaches its greatest value at the transitional radius. Since the shear stress on the membrane surface is not constant the average shear stress, equation (2), is more representative in the case of the whole membrane which was used here. Since the model, equation (1), does not take into consideration the flow rate of the discontinuous phase, it is expected that the model will be closest to predicting the droplets produced using a very low flow rate, as shown in Fig. 5. Droplets produced

using the higher flow rate followed the same trend as the one produced at lower transmembrane flux: increase of rotation speed decreased the droplet size, but the sizes of droplets produced at the higher transmembrane flux caused deviation from the model. Two explanations of this phenomenon are possible. First, the detachment of the droplet is not instantaneous but requires a finite time t_{neck}, the necking time, during which an additional amount of dispersed phase flows into the droplet [36]. Therefore, the resultant droplet volume, V, is larger than the one estimated by the force balance model and can be expressed as [36]: $V = V_{crit}+(t_{neck}/k)(Q_d/N)$ where V_{crit} is the droplet volume predicted by the model, k is the fraction of active pores, Q_d is the total dispersed phase flow rate and N is the total number of pores in the membrane. For example the data in Fig. 5 obtained at 3185 L m^{-2} h^{-1}, the above equation gives values of t_{neck}/k in the range from 0.13 s at 1330 rpm to 2.6 s at 230 rpm. The fraction of active pores k usually ranges from 2 to 50%, which means that t_{neck} should vary from 0.003–0.07 s at 1330 rpm to 0.05–1.3 s at 230 rpm. Another reason for the deviation between the model predictions and experimental data is insufficient coverage of the droplet surface with surfactant molecules during formation of the drops. The model calculations are made using the equilibrium interfacial tension which is lower than the dynamic interfacial tension during drop formation. Less coverage of the droplet surface by surfactant leads to a greater interfacial tension force and the resultant droplet is larger. It is notable that the drop size produced compared to the membrane pore size is a factor of x10 at the lowest shear, and x3 at the highest shear. The latter value is commonly assumed for membrane emulsification processes; the data here supports this value when operating at high shear conditions.

Encapsulation efficiencies were calculated using equation (7) and were found to be greater than 90% in all cases, and 98% at best. Images of fresh and 15 day old W/O/W emulsion with pumpkin seed oil are shown in Fig. 6, together with information on drop size and encapsulation efficiency. In the case of the variation of 'encapsulation efficiency' with time, this data represents the controlled release of the marker species from the internal water phase into the external water phase. Different shades of the grey, illustrated in the droplet images in Fig 6, demonstrate that the finely dispersed inner water droplets have substantially disappeared from the oil phase. This is consistent with the measured release of the copper leading to the reduction in 'encapsulation efficiency' with respect to time. There is only very limited change in drop size, from 176 to 172 μm at 0 to 15 days respectively. Also, with the exception of the span at 15 days the remaining spans are reasonably consistent. Hence, it appears that the drop size, and span, are stable for at least 12 days and possibly over the entire period of the test: 15 days. From this, it would appear that the mechanism for release of the internal phase is not simply W/O/W drop instability. Further analysis was performed on another lipid material forming W/O/W emulsion: refined sunflower oil, to remove undue influence from the minor components in the unrefined pumpkin seed oil.

In Fig. 7 the release of copper into the exterior water phase is presented in terms of encapsulation efficiency with respect to time. Three different rotation speeds were used to generate the W/O/W emulsion: giving drop sizes of 165, 107 and 92 μm at paddle rotation speeds of 900, 1200 and 1500 rpm respectively. At the higher drop sizes there appears to be a period during which there is only very limited release, which is similar to what is illustrated in Fig. 6: where the encapsulation efficiency is

constant for 6 days. At the smaller size illustrated in Fig. 7 (i.e. 92 μm) this initial period does not exist. However, the release profile is clearly not simply diffusion based: Fig. 7 has a model release curve included based on equation (3) using an extremely low (best fit to the data) effective diffusion coefficient of 2×10^{-16} m^2 s^{-1}. The data clearly does not fit the diffusional curve very well, and the data illustrated by the larger sizes is an even poorer fit to a diffusion curve. It is notable that the release rate is higher with smaller drop size, as would be expected for an interfacial area based transfer mechanism, but even a simple mass transfer coefficient based model would provide a release curve, unlike the near-linear release rate obtained from the smallest size, and the delayed release curves obtained at the larger drop sizes.

Conclusions

The Dispersion Cell and flat disc nickel membranes was used to produce narrow size distribution droplets of multiple emulsions containing unrefined pumpkin seed oil with controllable volume median diameters from 100 to 430 μm. For most of the work, membranes with 20 and 40 μm pores with 200 μm pore spacing were used, and it was possible to obtain fluxes up to 3200 L m^{-2} h^{-1} while the span in most cases did not exceed 0.5. Extreme cases (low rotation speed and high flux as well as high rotation speed and low flux) were not optimal conditions for production of multiple emulsions and in these few cases the span was higher.

The reproducibility of the experiments was good, showing no irreversible adsorption of the molecules of either surfactant, or oil component, onto the membrane surface,

and that after each experiment the membrane surface could be easily cleaned fully regaining its hydrophilicity.

Smaller droplets were produced using Tween 20 as a surfactant to stabilise the W/O/W emulsion than Pluronic F68, which was attributed to the lower interfacial tension and the more rapid diffusion of the Tween molecules and, therefore, shorter time needed for stabilizing the forming droplets.

Shear stress is the most effective way to regulate the droplet size: with an increase of the rotation speed by 5.7 times the droplet size decreased 2.6 times for a given membrane pore size. To measure the encapsulation efficiency, and the release rate, copper was encapsulated in the internal water phase. In all experiments the initial encapsulation efficiency was more than 94%. After 15 days encapsulation efficiency for the biggest droplets was 7.5 times higher than for the smallest droplets due to the smaller surface area through which copper could be released. However, the mechanism for release of the internal phase is complex: for the larger sizes there is a significant initial period with no release, followed by a roughly linear region of release with respect to time. For the smaller drops, less than 100 μm, the initial period of zero release was not observed. This pattern was observed for both W/O/W emulsions using refined sunflower oil as well as unrefined pumpkin seed oil. Visual observation of the W/O/W drops confirmed significant presence of fine internal phase water drops just after production of the emulsion, and almost clear drops after 15 days of release. The measured drop sizes, and spans, did not vary substantially during this period. Hence, it is concluded that the release mechanism is not one of unstable W/O/W drops and not simple diffusion from within the W/O/W droplet.

It has been demonstrated that the Dispersion Cell, with its mild conditions for generating the droplets, represents an effective tool for production of multiple emulsions containing this type of oil and very high entrapment efficiencies were obtained.

Acknowledgements

This research was part of the Integrated and Interdisciplinary Research Project No. 46010, financed by R. Serbia, 2011-2014. The authors wish to thank Alsu Aminova for conducting the encapsulation experiments with copper.

List of symbols

C_e	Copper concentration measured in the external aqueous phase of the $W_1/O/W_2$ emulsion after emulsification, kg m^{-3}
C_i	C_i is the copper concentration in the internal aqueous phase of the W/O emulsion, kg m^{-3}
d(v, 0.1)	Volume diameter below which smaller droplets constitute 10% of the total volume, m
d(v, 0.5)	Volume median diameter below which smaller droplets constitute 50% of the total volume, m
d(v, 0.9)	Volume diameter below which smaller droplets constitute 90% of the total volume, m
D_{eff}	'Effective' diffusion coefficient for the transferring species within the drop, m^2 s^{-1}

D_m	effective diameter of the membrane, m
k	Fraction of active pores, -
M_e	Mass of copper present in the external water phase in the W/O/W emulsion after homogenization, kg
M_i	Mass of copper present in the internal water phase in the W/O emulsion, kg
N	Total number of pores in the membrane, -
O_p	Pumpkin seed oil
O_s	Sunflower oil
q	Concentration of the encapsulated species, g g^{-1}
Q_d	Total dispersed phase flow rate, m^3 s^{-1}
r	Distance from the membrane centre, m
r_{trans}	Transitional radius, m
r_x	Radial position within the particle (or W/O/W composite drop), m
t	Time, s
t_{neck}	Necking time, s
V	Resultant droplet volume, m^3
V_{crit}	Droplet volume predicted by the model, m^3
V_e	Volume of external aqueous phase, m^3
V_i	Volume of internal aqueous phase, m^3
V_{WOW}	Volume of whole emulsion, m^3
x	Droplet diameter, m
Y	Encapsulation efficiency, -

Greek symbols

ρ	Continuous phase density, kg m^{-3}
γ	interfacial tension, N m^{-1}
ω	Angular velocity, rad s^{-1}
μ	Continuous phase coefficient of dynamic viscosity, Pa s
τ_{av}	Average shear stress, Pa
δ	Boundary layer thickness, m
ϕ_{WO}	Volume fraction of water droplets in the W_1/O emulsion, -
ϕ_{WOW}	Volume fraction of W/O droplets in the W/O/W emulsion, -

References

[1] W. Seifriz, Studies in emulsions, J. Phys. Chem., 29 (1925) 587–600.

[2] M. Nakano, Places of emulsions in drug delivery, Adv. Drug Deliv. Rev. 45 (2000) 1–4.

[3] T.V. Vasudevan and M.S. Naser, Some Aspects of Stability of Multiple Emulsions in Personal Cleansing Systems, J.Colloid Interface Sci. 256 (2002) 208–215.

[4] Z.M. Merchant, A.G. Gaonkar, V.J. Nicholson, and H.M. Tufts, Flavor delivery system, EP 815743 A3, 1998.

[5] D.G. Dalgleish, Food emulsions—their structures and structure-forming properties, Food Hydrocoll. 20 (2006) 415–422.

[6] S. Okonogi, R. Kato, Y. Asano, H. Yuguchi, R. Kumazawa, K. Sotoyama, et al, US Patent 5279847 1994.

[7] W. Daisuke, I. Noriko, and U. Akira, Fat-soluble vitamins-containing food and drink product, and method for stabilizing fat-soluble vitamins, JP2004097113 A, 2004.

[8] R.K. Owusu, Q. Zhu, and E. Dickinson, Controlled release of L-tryptophan and Vitamin B2 from model water/oil/water multiple emulsions, Food Hydrocoll. 6 (1992) 443–453.

[9] C.C. Chen, Y.Y. Tu, and H.M. Chang. Efficiency and protective effect of encapsulation of milk immunoglobulin G in multiple emulsion. J. Agric. Food Chem. 47 (1999) 407.

[10] F. Cournarie, M. Savelli, V. Rosilio, F. Bretez, C. Vauthier, J. Grossiord, et al., Insulin-loaded W/O/W multiple emulsions: comparison of the performances of

systems prepared with medium-chain-triglycerides and fish oil, Eur. J. Pharm. Biopharm. 58 (2004) 477–482.

[11] J. Weiss, I. Scherze, and G. Muschiolik, Polysaccharide gel with multiple emulsion, Food Hydrocoll. 19 (2005) 605–615.

[12] Y.H. Cho and J. Park, Evaluation of process parameters in the O/W/O multiple emulsion method for flavor encapsulation, J. Food Sci. 68 (2003) 534–538.

[13] G. Muschiolik, Multiple emulsions for food use, Curr. Opin. Coll. Int. Sci. 12 (2007) 213–220.

[14] N. Garti, Double emulsions—scope, limitations and new achievements, Colloid. Surf. A 123 (1997) 233–246.

[15] S. van der Graaf, C.G.P.H. Schroën, and R.M. Boom, Preparation of double emulsions by membrane emulsification—a review, J. Membr. Sci. 251 (2005) 7–15.

[16] V. Schröder, O. Behrend, and H. Schubert, Effect of dynamic interfacial tension on the emulsification process using microporous, ceramic membranes, J. Colloid Interface Sci. 202 (1998) 334–340.

[17] S.R. Kosvintsev, G. Gasparini, and R.G. Holdich, Membrane emulsification: Droplet size and uniformity in the absence of surface shear, J. Membr. Sci. 313 (2008) 414–420.

[18] T. Nakashima, M. Shimizu, and M. Kukizaki, Membrane emulsification by microporous glass, Key Eng. Mat. 61 (1992) 513–516.

[19] A.J. Gijsbertsen-Abrahamse, A. van der Padt, and R.M. Boom, Status of cross-flow membrane emulsification and outlook for industrial application, J. Membr. Sci. 230 (2004) 149–159.

[20] T.A. El-Adawy and K.M. Taha, Characteristics and composition of watermelon, pumpkin, and paprika seed oils and flours, J. Agric. Food Chem. 49 (2001) 1253–1259.

[21] D.G. Stevenson, F.J. Eller, L. Wang, J.L. Jane, T. Wang, and G.E. Inglett, Oil and tocopherol content and composition of pumpkin seed oil in 12 cultivars, J. Agric. Food Chem. 55 (2007) 4005–4013.

[22] T. Kawakatsu, G. Trägårdh, and C. Trägårdh, Production of W/O/W emulsions and S/O/W pectin microcapsules by microchannel emulsification, Colloid. Surf. A, 189 (2001) 257–264.

[23] U. Lambrich, S. van der Graaf, K. Dekkers, H. Schubert, and R.M. Boom, Production of double emulsions using microchannel emulsification, Proceedings of ICEF, 9 (2004).

[24] S. Sugiura, M. Nakajima, K. Yamamoto, S. Iwamoto, T. Oda, M. Satake, et al., Preparation characteristics of water-in-oil-in-water multiple emulsions using microchannel emulsification, J. Colloid Interface Sci. 270 (2004) 221–228.

[25] T. Thorsen, R.W. Roberts, F.H. Arnold, and S.R. Quake, Dynamic pattern formation in a vesicle-generating microfluidic device, Phys. Rev. Lett. 86 (2001) 4163–4166.

[26] A.M. Gañán-Calvo and J.M. Gordillo, Perfectly monodisperse microbubbling by capillary flow focusing, Phys. Rev. Lett. 87 (2001) 274501.

[27] M.M. Dragosavac, M.N. Sovilj, S.R. Kosvintsev, R.G. Holdich, and G.T. Vladisavljević, Controlled production of oil-in-water emulsions containing unrefined pumpkin seed oil using stirred cell membrane emulsification, J. Membr. Sci. 322 (2008) 178–188.

[28] R.G. Holdich, M.M. Dragosavac, G.T. Vladisavljević and S.R. Kosvintsev, Membrane Emulsification with Oscillating and Stationary Membranes, Ind. Eng. Chem. Res. 49 (2010) 3810–3817.

[29] G.T. Vladisavljević and H. Schubert, Influence of process parameters on droplet size distribution in SPG membrane emulsification and stability of prepared emulsion droplets, J. Membr. Sci. 225 (2003) 15–23.

[30] J. Surh, G.T. Vladisavljević, S. Mun, and D.J. McClements, Preparation and characterization of water/oil and water/oil/water emulsions containing biopolymer-gelled water droplets, J.Agric.Food Eng. 55 (2007) 175–184.

[31] G.T. Vladisavljević and H. Schubert, Preparation and analysis of oil-in-water emulsions with a narrow droplet size distribution using Shirasu-porous-glass (SPG) membranes, Desalination 144 (2002) 167–172.

[32] J. Tong, M. Nakajima, H. Nabetani, and Y. Kikuchi, Surfactant effect on production of monodispersed microspheres by microchannel emulsification method, J Surfactants Deterg. 3 (2000) 285–293.

[33] S. van der Graaf, C.G.P.H. Schroën, R.G.M. van der Sman, and R.M. Boom, Influence of dynamic interfacial tension on droplet formation during membrane emulsification, J. Colloid Interface Sci. 277 (2004) 456–463.

[34] R. Soong, M.P. Nieh, E. Nicholson, J. Katsaras, and P.M. Macdonald, Bicellar mixtures containing Pluronic F68: morphology and lateral diffusion from combined SANS and PFG NMR studies, Langmuir 26 (2010) 2630–2638.

[35] F. Luschtinetz and C. Dosche, Determination of micelle diffusion coefficients with fluorescence correlation spectroscopy (FCS), J. Colloid Interface Sci. 338 (2009) 312–315.

[36] S. van der Graaf, T. Nisisako, C.G.P.H. Schroën, R.G.M. van der Sman, and

R.M. Boom, Lattice Boltzmann simulations of droplet formation in a T-shaped microchannel, Langmuir 22 (2006) 4144–4152.

[37] S.R. Kosvintsev, G. Gasparini, R.G. Holdich, I.W. Cumming, and M.T. Stillwell. Liquid− Liquid Membrane Dispersion in a Stirred Cell with and without Controlled Shear. Ind Eng Chem Res, 44 (2005) 9323.

[38] J.H. Xu, G.S. Luo, G.G. Chen, and J.D. Wang. Experimental and theoretical approaches on droplet formation from a micrometer screen hole. J.Membr.Sci., 266 (2005) 121.

List of tables

Table 1 The composition of $W_1/O/W_2$ emulsions prepared

Inner aqueous phase, W_1	Pure Milli - Q water
Oil phase	5 wt.% PGPR dissolved in unrefined pumpkin seed oil (O_p) or refined sunflower oil (O_s)
Outer aqueous phase, W_2	2 wt.% Tween® 20 dissolved in Milli–Q water, in some experiments PVA was added
Volume percent of inner aqueous phase in W_1/O emulsion (vol.%)	φ_i=0 or 30
Volume percent of W_1/O emulsion drops in $W_1/O/W_2$ emulsion (vol.%)	φ_o=5
Mean size of outer drops	102-422 and 134-433 μm for the pore size of 20 and 40 μm, respectively

Table 2 Density and viscosity of aqueous surfactant solutions used work and measured equilibrium interfacial tension at oil/aqueous phase interface

Aqueous phase	**Density (kg/m^3)**	**Viscosity (mPa s)**	**Oil phase**	**Interfacial tension (mN/m)**
2 wt. % Tween	1000	1.01	Unrefined pumpkin seed oil (O_p)	1.5
2 wt. % Tween			W/O_p	1.0
2 wt. % Pluronic F-68	1000	1.28	O_p	6.0
2 wt. % Pluronic F-68			W/O_p	3.7
2 wt. % Pluronic F-68			O_p + 5% PGPR	3.0
Demineralised water	997	0.891		11
2 wt. % Tween	1000	1.01	Refined sunflower oil (O_s)	5.0
2 wt. % Tween			W/O_s	0.83
Demineralised water	997	0.891		22

List of figures

Fig. 1 Photomicrograph of 20 μm membrane and schematic illustration of Dispersion Cell with simple paddle used (b = 12 mm, D = 32 mm, D_m = 33 mm, n_b = 2, and T = 40 mm)

Fig. 2 Variation of volume median diameter and span of particle size distribution with dispersed phase flux for the membrane with 20 μm pore size; disperse phase: water-in-pumpkin seed oil, continuous phase: 2% Tween 20 and, for comparison, one 40 μm pore size membrane at 600 rpm. Open symbols predict the droplet size using the model: equation (1) when the flux is zero.

Fig. 3 Effect of PGPR and internal water phase on the droplet size and appearance in 4 consecutive sets of experiments with the same membrane. Disperse phase: 1: Pure pumpkin seed oil (O_p); 2: 5% PGPR dissolved in pumpkin seed oil; 3: W/O_p emulsion with 30% water phase and 5% PGPR in pumpkin seed oil, and 4: Experiment with pure pumpkin seed oil performed after previous experiments. Pore size = 15 μm, pores spacing = 200 μm, transmembrane flux = 600 L m^{-2} h^{-1}, rotation speed = 600 rpm, continuous phase: 2% Pluronic F68

Fig. 4 Variation of volume median diameter and span of particle size distribution with dispersed phase flux for 2% surfactant solutions (disperse phase: water-in-pumpkin seed oil, pore size = 20 μm, rotation speed = 600 rpm)

Fig. 5 Experimental drop diameters of water-in-(pumpkin seed oil)-in-water multiple emulsions produced; pore size = 40 μm, continuous phase: 2% Tween 20, solid line represents the force balance model: equation (1), for near zero flux.

Fig. 6 (a) (●) Encapsulation efficiency of copper for $W/O_2/W$ emulsion and (▲) mean droplet diameter for 15 days stored at room temperature. Pore size = 20 μm, rotation speed = 960 rpm, transmembrane flux = 640 L m^{-2} h^{-1}. (b) (★) Span of particle size distribution over 15 days

Fig. 7 Encapsulation efficiency of copper as a function of time for water-in-sunflower oil-in-water emulsion at room temperature. Transmembrane flux = 320 L m^{-2} h^{-1}. (▲) $d_{3,2}$=165 μm, d(v,0.5)=168 μm, span=0.33, (○) $d_{3,2}$=107 μm, d(v,0.5)=109 μm, span=0.44, (►) $d_{3,2}$=92 μm, d(v,0.5)=95 μm, span=0.47 and diffusion model for 92 μm drops

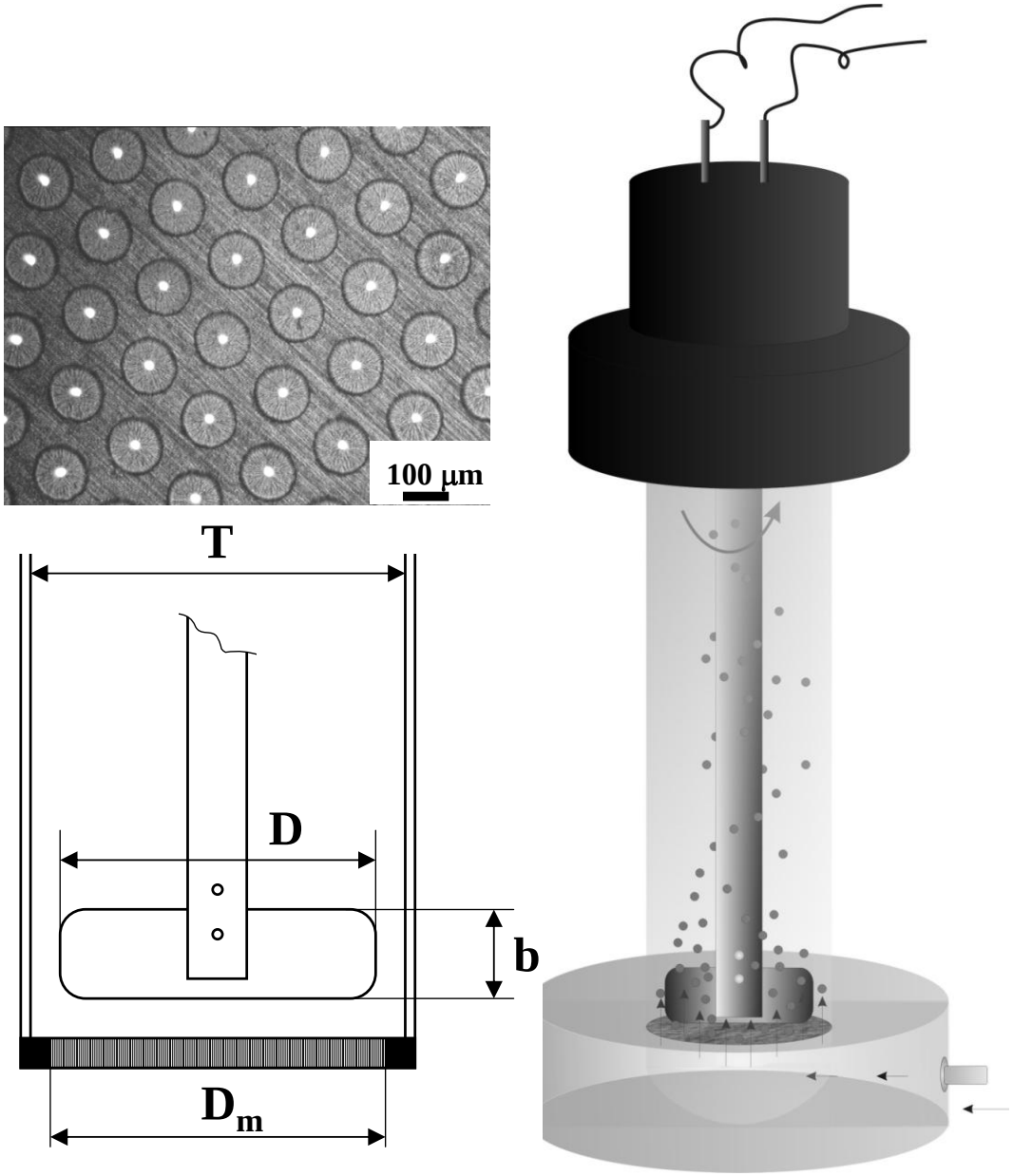

Fig. 1 Photomicrograph of 20 µm membrane and schematic illustration of Dispersion Cell with simple paddle used (b = 12 mm, D = 32 mm, D_m = 33 mm, n_b = 2, and T = 40 mm).

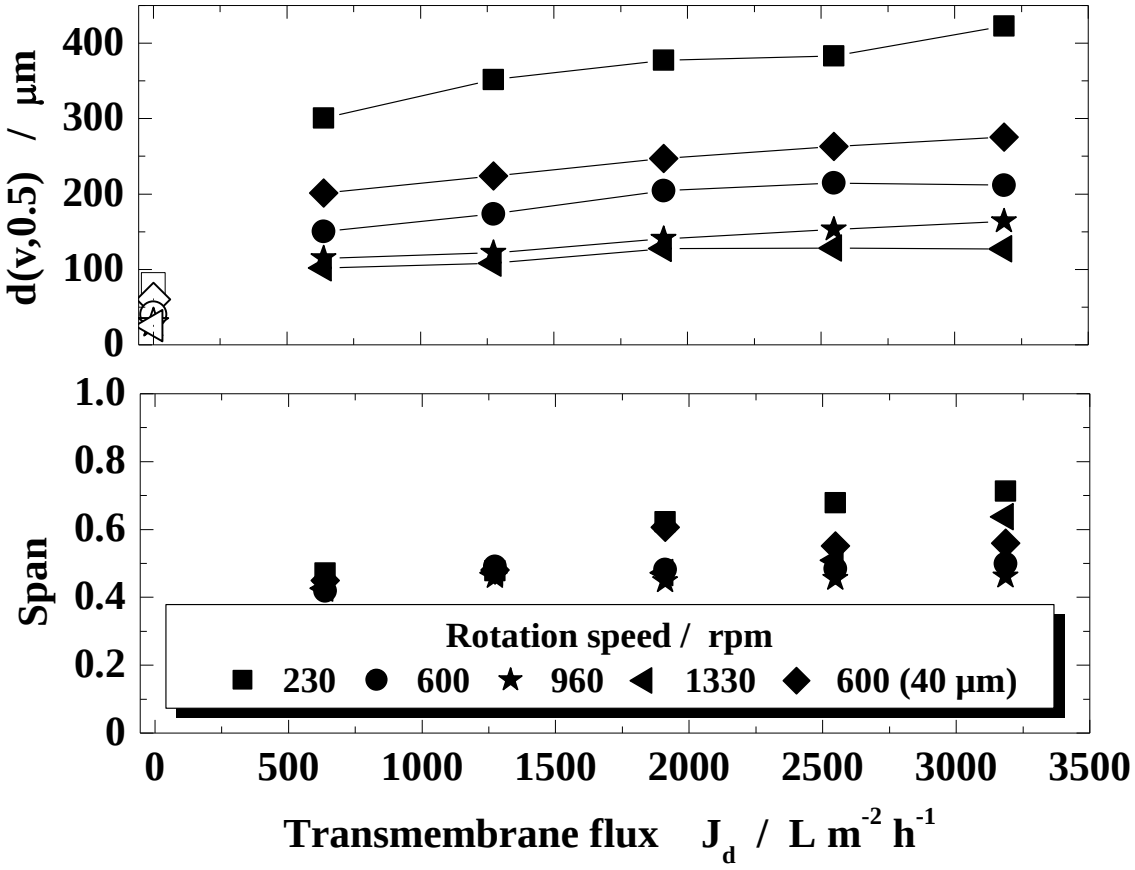

Fig. 2 Variation of volume median diameter and span of particle size distribution with dispersed phase flux for the membrane with 20 μm pore size; disperse phase: water-in-pumpkin seed oil, continuous phase: 2% Tween 20 and, for comparison, one 40 μm pore size membrane at 600 rpm. Open symbols predict the droplet size using the model: equation (1) when the flux is zero.

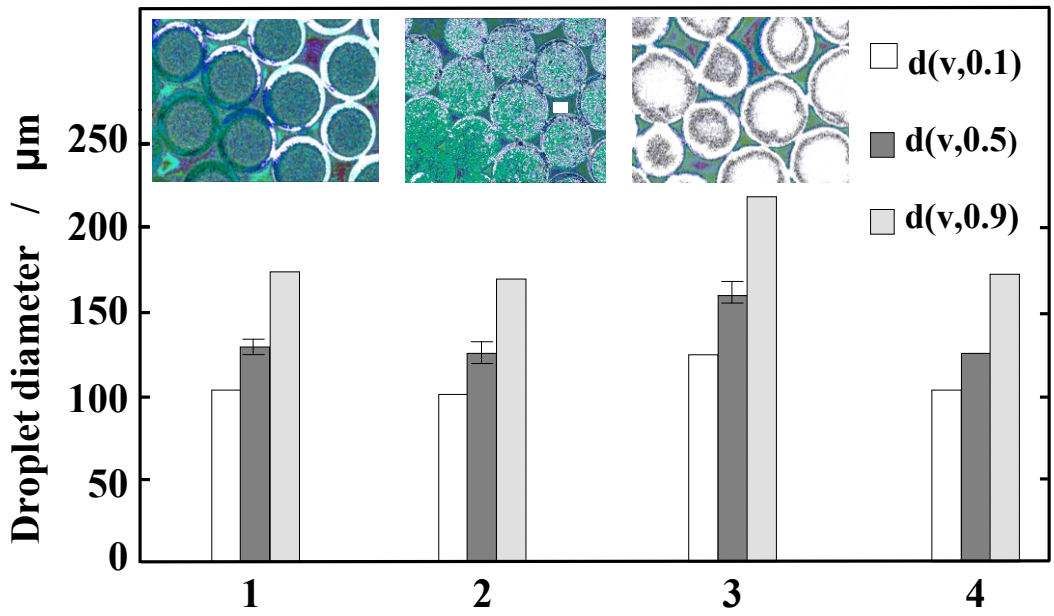

Fig. 3 Effect of PGPR and internal water phase on the droplet size and appearance in 4 consecutive sets of experiments with the same membrane. Disperse phase: 1: Pure pumpkin seed oil (O_p); 2: 5% PGPR dissolved in pumpkin seed oil; 3: W/O_p emulsion with 30% water phase and 5% PGPR in pumpkin seed oil, and 4: Experiment with pure pumpkin seed oil performed after previous experiments. Pore size = 15 µm, pores spacing = 200 µm, transmembrane flux = 600 L m^{-2} h^{-1}, rotation speed = 600 rpm, continuous phase: 2% Pluronic F68.

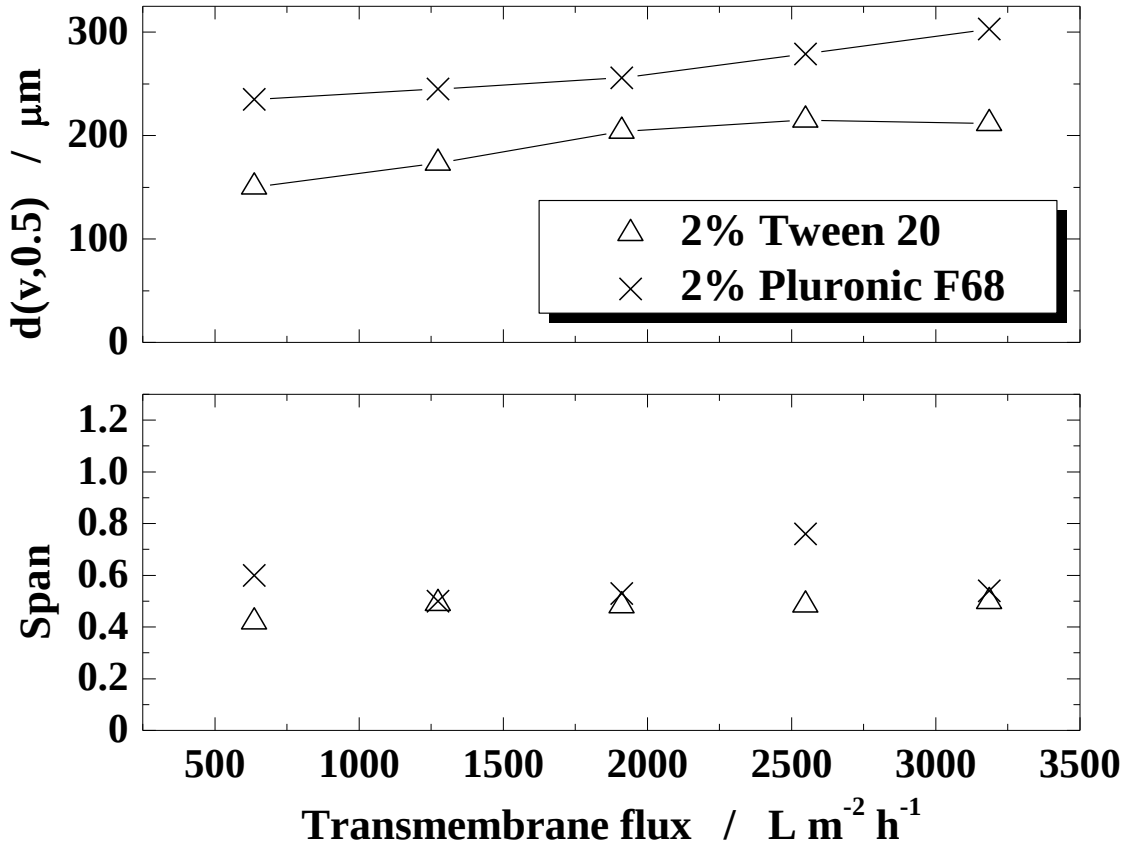

Fig. 4 Variation of volume median diameter and span of particle size distribution with dispersed phase flux for 2% surfactant solutions (disperse phase: water-in-pumpkin seed oil, pore size = 20 μm, rotation speed = 600 rpm).

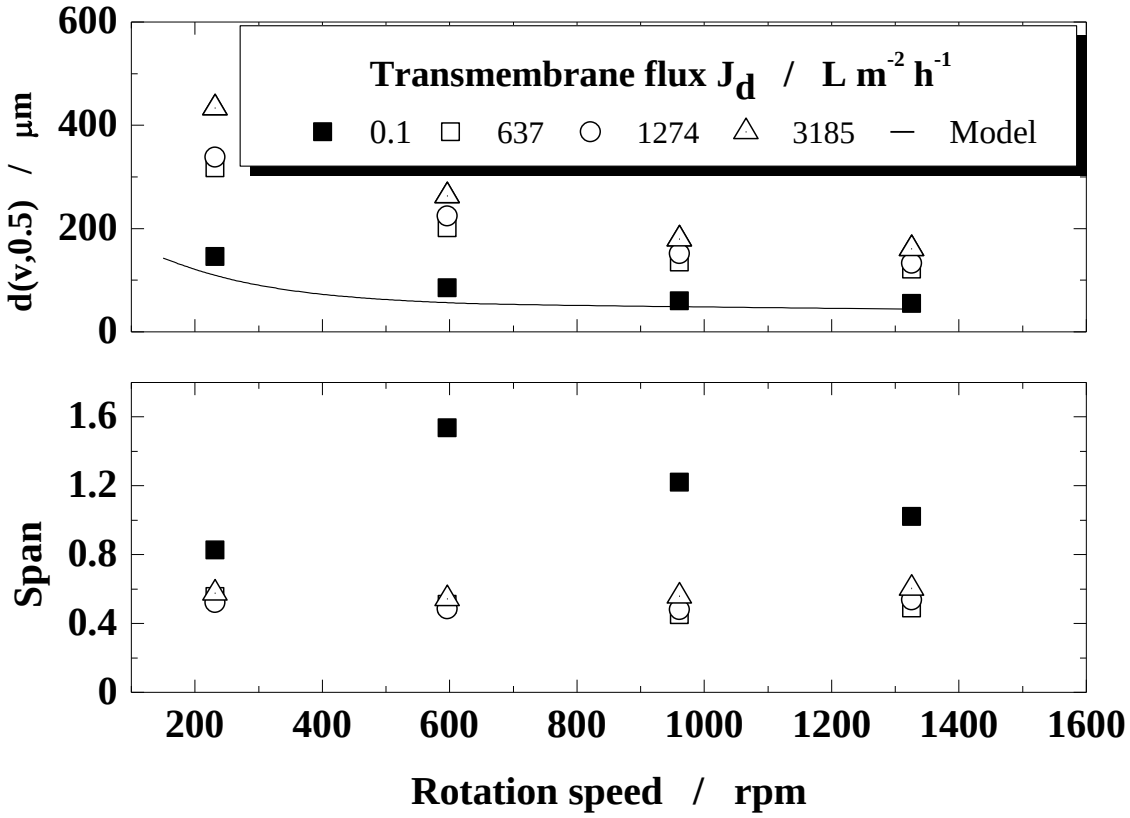

Fig. 5 Experimental drop diameters of water-in-(pumpkin seed oil)-in-water multiple emulsions produced; pore size = 40 µm, continuous phase: 2% Tween 20, solid line represents the force balance model: equation (1), for near zero flux.

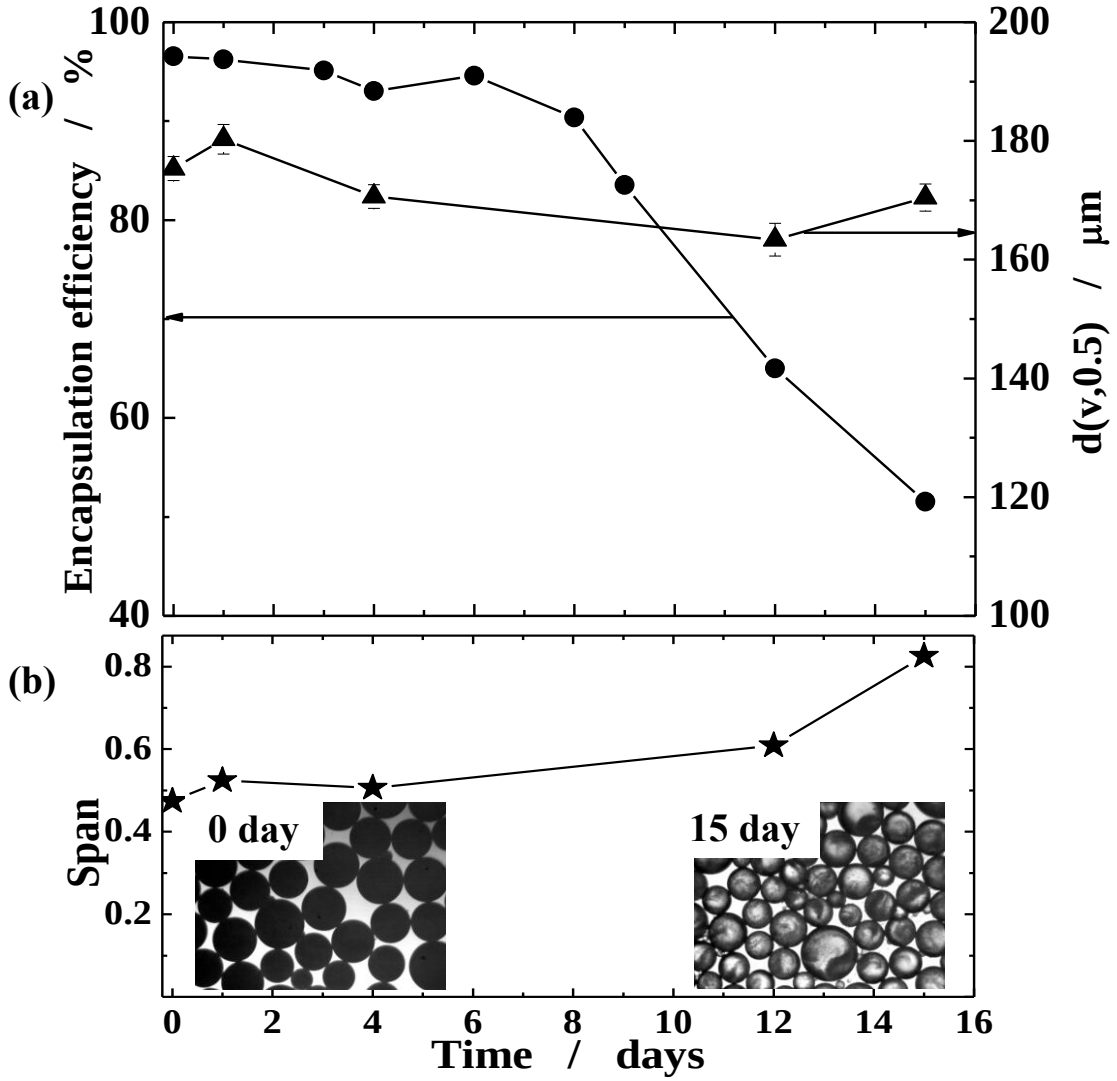

Fig. 6 (a) (●) Encapsulation efficiency of copper for $W/O_2/W$ emulsion and (▲) mean droplet diameter for 15 days stored at room temperature. Pore size = 20 μm, rotation speed = 960 rpm, transmembrane flux = 640 L m^{-2} h^{-1}. (b) (★) Span of particle size distribution over 15 days.

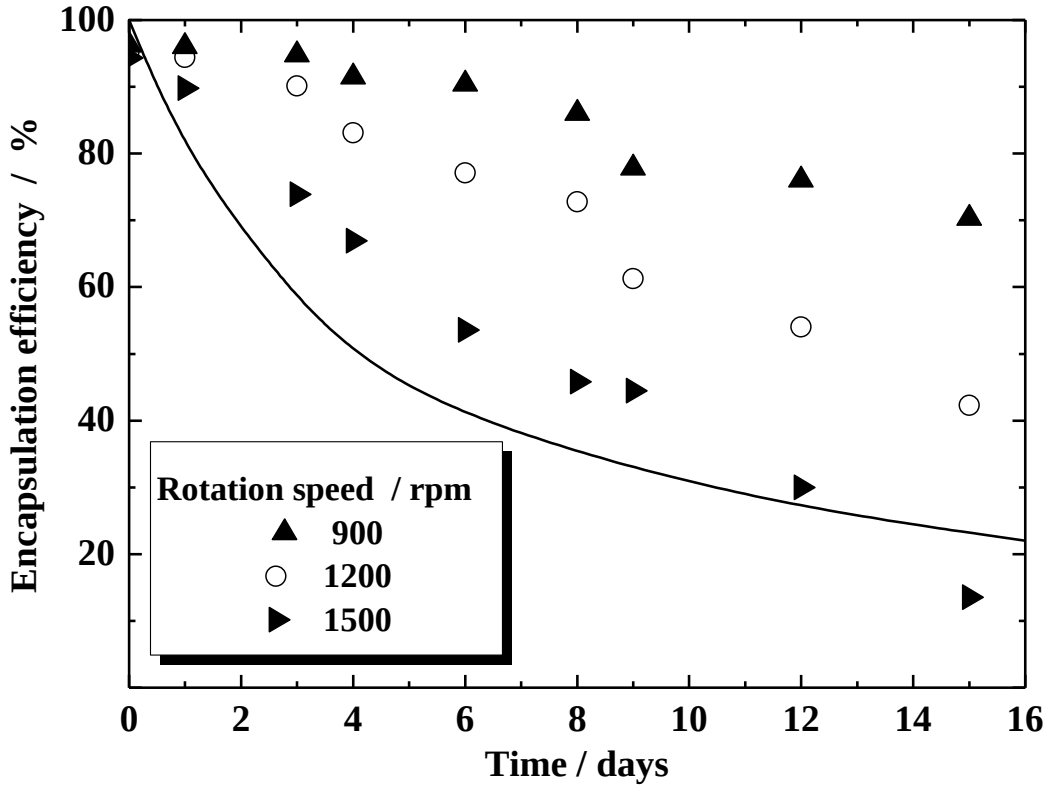

Fig. 7 Encapsulation efficiency of copper as a function of time for water-in-sunflower oil-in-water emulsion at room temperature. Transmembrane flux = 320 L m^{-2} h^{-1}. (▲) $d_{3,2}$=165 μm, $d(v,0.5)$=168 μm, span=0.33; (○) $d_{3,2}$=107 μm, $d(v,0.5)$=109 μm, span=0.44; (►) $d_{3,2}$=92 μm, $d(v,0.5)$=95 μm, span=0.47 and diffusion model for 92 μm drops.